Arab J Geosci (2015) 8:11073–11092
DOI 10.1007/s12517-015-1970-9

ORIGINAL PAPER

Sedimentological, mineralogical, and geochemical characterization of sand dunes in Saudi Arabia

Mohammed Benaafi[1] **· Osman Abdullatif**[1]

Received: 5 February 2015 / Accepted: 21 May 2015 / Published online: 16 June 2015
© Saudi Society for Geosciences 2015

Abstract This paper investigates the morphology, texture, composition, mineralogy, and geochemistry, and provenance of sand dunes from 10 locations in Saudi Arabia. Morphologically, these sand dunes include linear, parallel to subparallel ridge, parabolic, barchans, and star sand dunes. Sixty-seven samples were collected from these different sand dune types. Generally, sands from dunes in all locations were characterized by fine to coarse mean grain size, were moderately sorted, and had near symmetrical skewness with mesokurtic distribution. Skewness and mesokurtic distribution characterize sand dunes in most locations except the Red Sea, Qassim, central Arabia, and the Eastern Province where sand dunes all show of subangular grains. The sand dunes are composed of quartz, feldspar, calcite, and mica. Quartz dominates the mineralogy of all sand dunes, although significant amounts of feldspars and mica are found in Najran, the Red Sea, and Central Arabia. While calcite is present in sand dunes at Sakaka and NW Rub' Al-Khali. Basement-related sand dunes at Najran (N1), central Arabia (C5), and the Red Sea are mineralogically submature. However, nonbasement sand dunes at other locations are mature. Both petrographic and geochemical analyses of sand dunes indicated that most sand dunes are classified as quartz arenite, except in the basement-related sand dunes at Najran (N1), central Arabia (C5), and the Red Sea, where they range from subarkose to litharenite. Moreover, major, trace, and rare earth elements indicated an active continental margin tectonic setting for sand dunes from the Red Sea, basement-related Najran (N1), and central Arabia (C5) sand dunes, and passive continental margins for the other locations.

Keywords Sand dunes · Sedimentology · Provenance · Tectonics · Saudi Arabia

Introduction

More than 50 % of the land surface in Saudi Arabia is occupied by sand dunes, distinct geomorphological features in the country. There are four major deserts in Saudi Arabia: An Nafud, the Dahna, the Rub' Al-Khali, and Jafurah in the eastern part. The sand dunes in Saudi Arabia occur in arid desert regions as well as the Arabian Gulf and Red Sea coastal plains.

Inland and coastal sand dunes in desert environments are texturally and compositionally controlled by chemical and physical processes such as wind action, fluvial and marine processes, weathering, precipitation, and air temperature (Muhs 2004). Grain size variations in desert and coastal sand dunes have been commonly used to understand transport and depositional mechanisms (Wang et al. 2003). Poorly to moderately sorted sand dunes occur within a short transport distance and close proximity to the source area of sediments (Blount and Lancaster 1990). However, a longer eolian transport path creates better sorted and fine-grained sand dunes (Kasper-Zubillaga and Carranza-Edwards 2005). In addition, mineralogical and geochemical studies of sand dunes offer new insights into the origin and evolution of eolian sand dunes (Muhs 2004). Quartz-rich sand dunes are mineralogically mature and may inherit their composition from sandstone rich in quartz, as well as weathered plutonic and metamorphic rocks. Maturity of dune sands might also be related to the depletion of unstable minerals such as feldspars through chemical weathering, ballistic impacts in high energy eolian environments, and fluvial size reduction of feldspars (Muhs 2004). However, while dune sands rich in feldspars may be derived

✉ Mohammed Benaafi
benaafi@kfupm.edu.sa

[1] Earth Sciences Department, KFUPM, Dhahran, Saudi Arabia

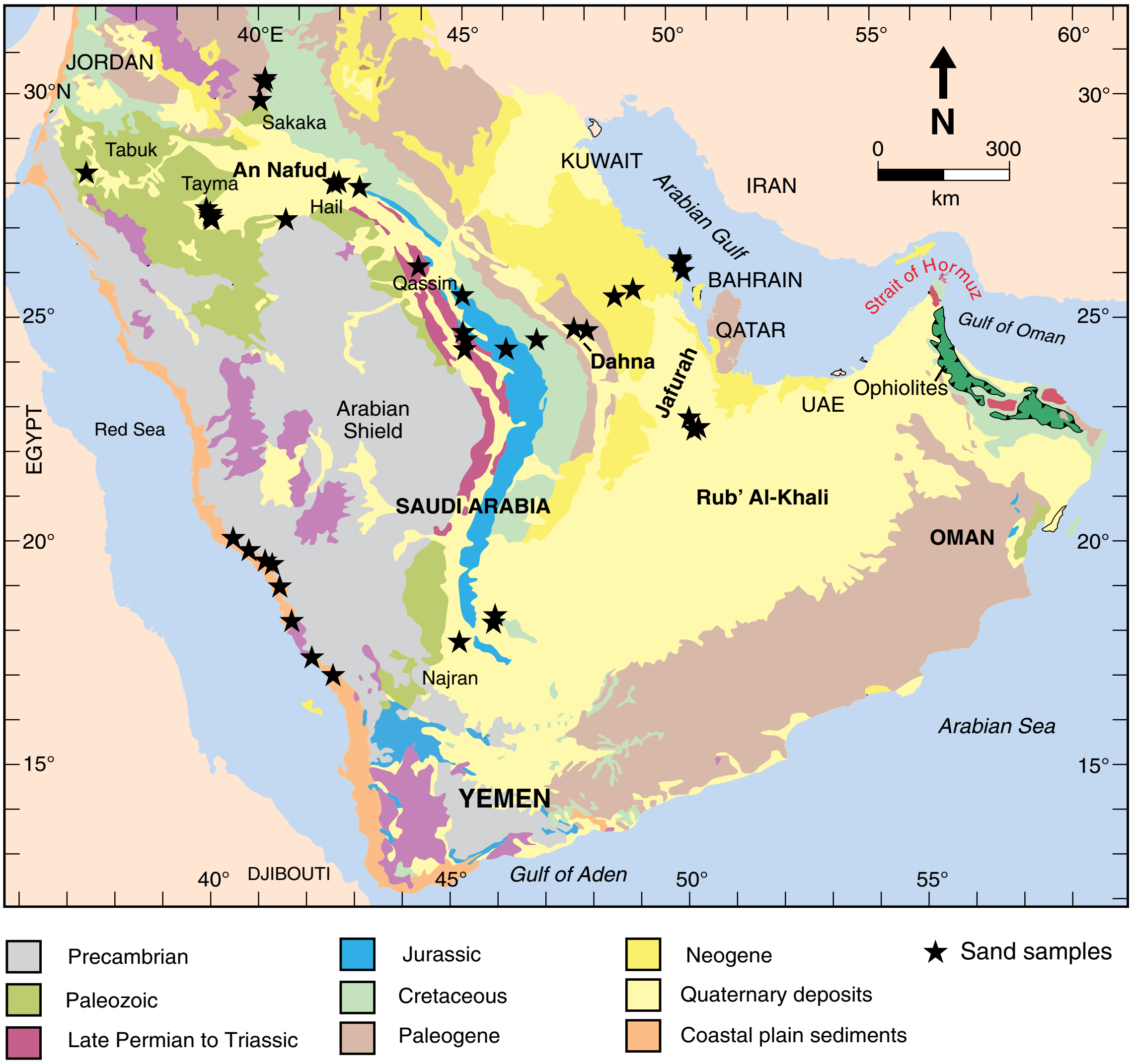

Fig. 1 Geological map of Arabian Peninsula shows the area of the study and locations of sand samples (modified after Le Nindre et al. 2003 and Issautier et al. 2012)

from feldspar-rich source rock (arkosic sources), they may also be the result of minimal chemical weathering and the short transport distance of eolian sediments (Muhs 2004).

Early studies of sand dunes in the Arabian deserts were performed by Phillips (1982). Sagga (1998) studied the roundness of sand grains in longitudinal sand dunes in the western region of Saudi Arabia, and Jafurah sand dunes in the eastern region of Saudi Arabia have been studied by Fryberger et al. (1984). Anton (1983) studied the evolution of modern eolian deposits in the Eastern Province, including Jafurah, Dahna, and Rub' Al-Khali. Grain size distributions of dune sands from An Nafud Rahmat and Wadi Khulays have been studied by Binda (1983), and grain size distributions of Barchans dune sands from Al-Ubaylah in the northwest part of Rub' Al-Khali have been studied by Abolkhair (1986). Watson (1986) analyzed variations in grain sizes from longitudinal dune sands taken from the center of the Namib Desert and Barchans dune sands from the Jafurah Desert in Saudi Arabia. Sagga (1998) studied the geomorphology and sedimentology of Barchans dunes from Wadi Khulays in the western region of Saudi Arabia. Al-Masrahy and Mountney (2013) studied the morphology of sand dunes in Rub' Al-Khali using remote sensing techniques, and, recently, Moufti (2013) studied the homogeneity of the mineral composition and variations in grain size in dunes in the Western part of Rub' Al-Khali.

Regionally, sand dune seas have been studied in Oman, UAE, and Yemen. Pease et al. (1999) studied the mineralogical characterizations and transport pathways in the Wahiba sand seas of Oman using remote sensing, while the history of the coastal Wahiba sand dunes has been studied by Preusser et al. (2005). Al-Sayed (1999) studied the sedimentology and morphology of sand dunes in the eastern part of UAE. Variations in texture among four types of sand dunes within Kuwait have been studied by Al-Dousari et al. (2008), while the

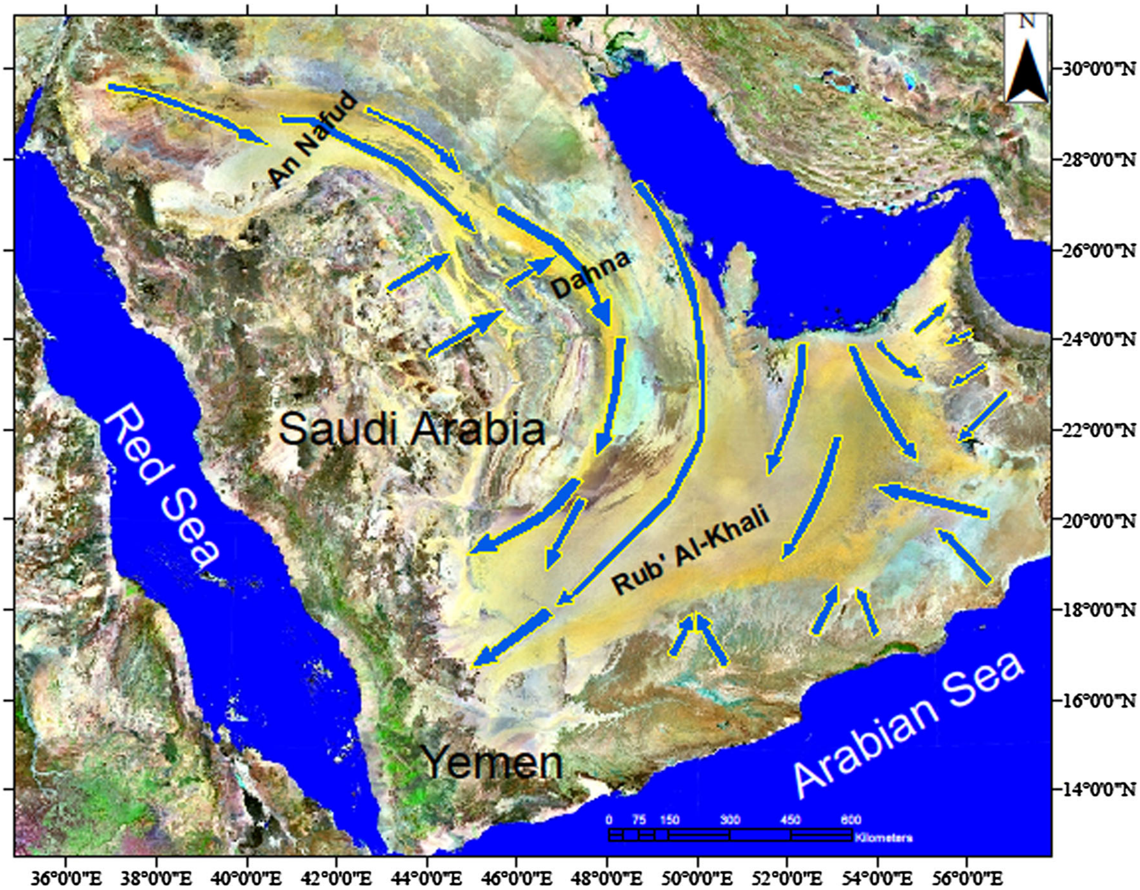

Fig. 2 Satellite image shows the paleo direction of eolian sand movement during Quaternary time modified after Edgell (2006)

provenance and recycling of dune sands across Saudi Arabia, Oman, UAE, and Yemen have been investigated by Garzanti et al. (2003, 2013).

This study aims to determine the sedimentological, mineralogical, geomorphological, and geochemical differences among sand dunes in different locations within Saudi Arabia and to establish the provenance and tectonic setting of these sand dunes.

Materials and methods

Study area

The study areas include sand dunes in 10 locations within Saudi Arabia. These locations include NW part of Rub' Al-Khali, Najran (western part of Rub' Alkhali desert), central Arabia, Qassim, Hail, Tayma, Tabuk, Sakaka, the Eastern Province (Al-Lidam and the Arabian Gulf coastal dunes), and the Red Sea (Fig. 1). Sand dunes at Najran area are bordered in the west by Paleozoic age sedimentary rocks (Wajid Sandstone). These sand dunes are cut across by a small ridge of the Jurassic age Tawiaq Mountain (limestone) trending N–S. The Rub' Al-Khali sand dunes south of Al-Ahsa city are bordered by Quaternary age deposits from all directions. Sand dunes in the Red Sea coastal plain, from Jizan city in the southern part of Saudi Arabia northward to Jeddah city, are bordered by Precambrian basement rock mountains from the east and the Red Sea from the west. In central Arabia, west of Riyadh city, sand dunes are located between the Jurassic Tawiaq Mountain and Late Permian to Triassic age sedimentary rock outcrops and within the Late Permian to Triassic sedimentary rock outcrops. Sand dunes in the Qassim area are surrounded by Paleozoic age sedimentary rock outcrops and Late Permian to Triassic sedimentary age outcrops. In the Dahna desert east of Riyadh city, sand dunes are bordered from the NE and SW by Tertiary age sedimentary outcrops and extend NW and SE. Sand dunes in An Nafud Desert in the northern part of Saudi Arabia in Hail area are bordered on the NE by Jurassic/Cretaceous age and Precambrian age outcrops and by Paleozoic age outcrops from the South and SW. In the Tayma area, sand dunes of An Nafud desert are surrounded by Paleozoic age outcrops from all sides

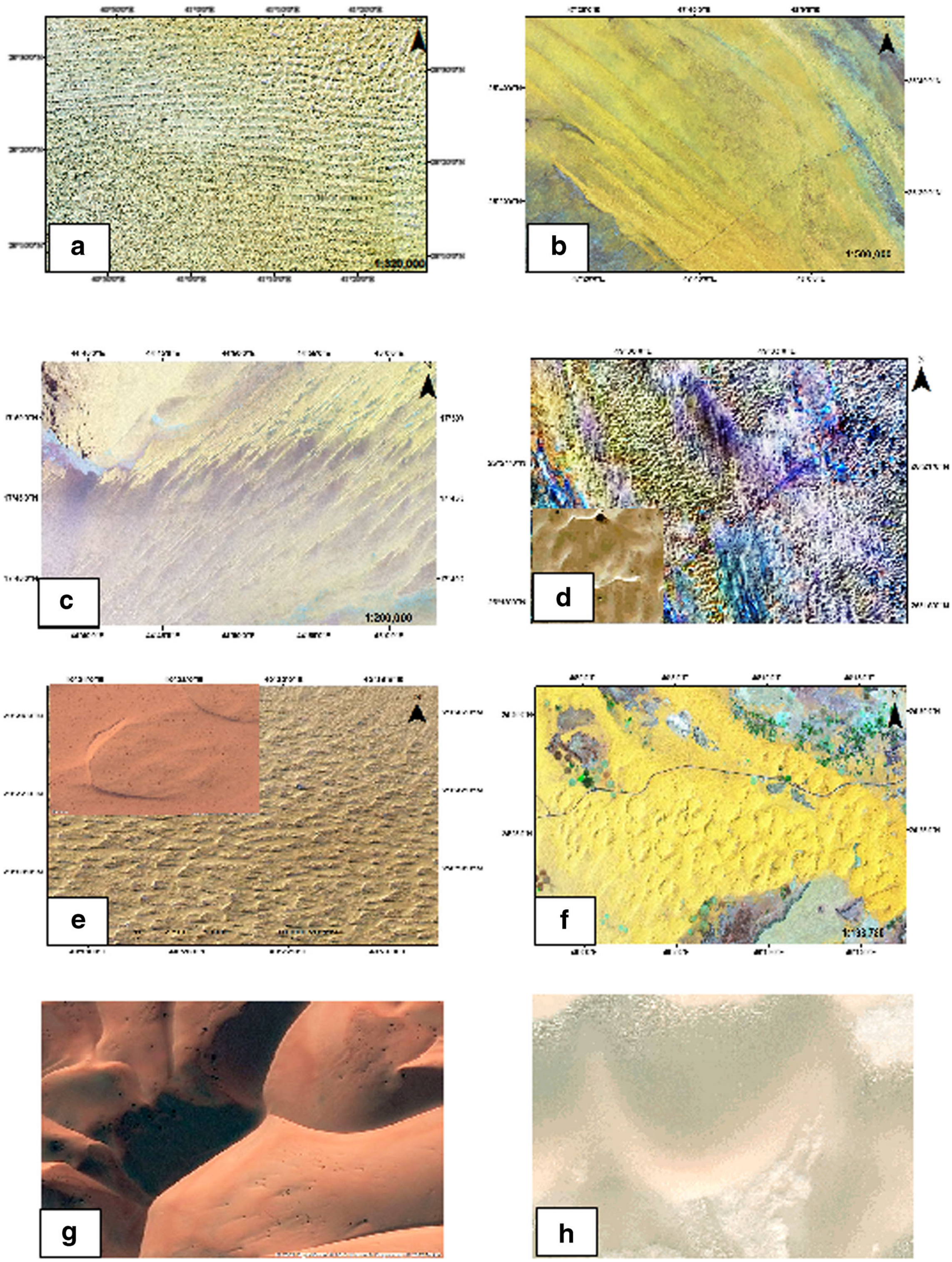

Fig. 3 Landsat image of Saudi sand dunes. **a** Linear sand ridges with E–W direction (An Nafud desert, Hail area). **b** Linear sand ridges with NW–SE direction (Dahna desert, central Arabia). **c** Linear sand ridges with NE–SW direction [Rub' Al-Khali desert (Najran area)]. **d** Linear sand ridges and transverse dune type with NE–SW direction (Al-Lidam area, Eastern Province). **e** Parabolic sand dunes (An Nafud desert (Hail area). **f** Dome sand dunes. Central Arabia desert (Al-Muzahamiah town). **g** Star sand dunes in Dahna desert. **h** Barchan sand dunes in Jafurah desert

except the NE. In the Sakaka area, sand dunes are located within Tertiary outcrops. Finally, in the Tabuk region, sand dunes are located within Paleozoic sedimentary outcrops (Fig. 1).

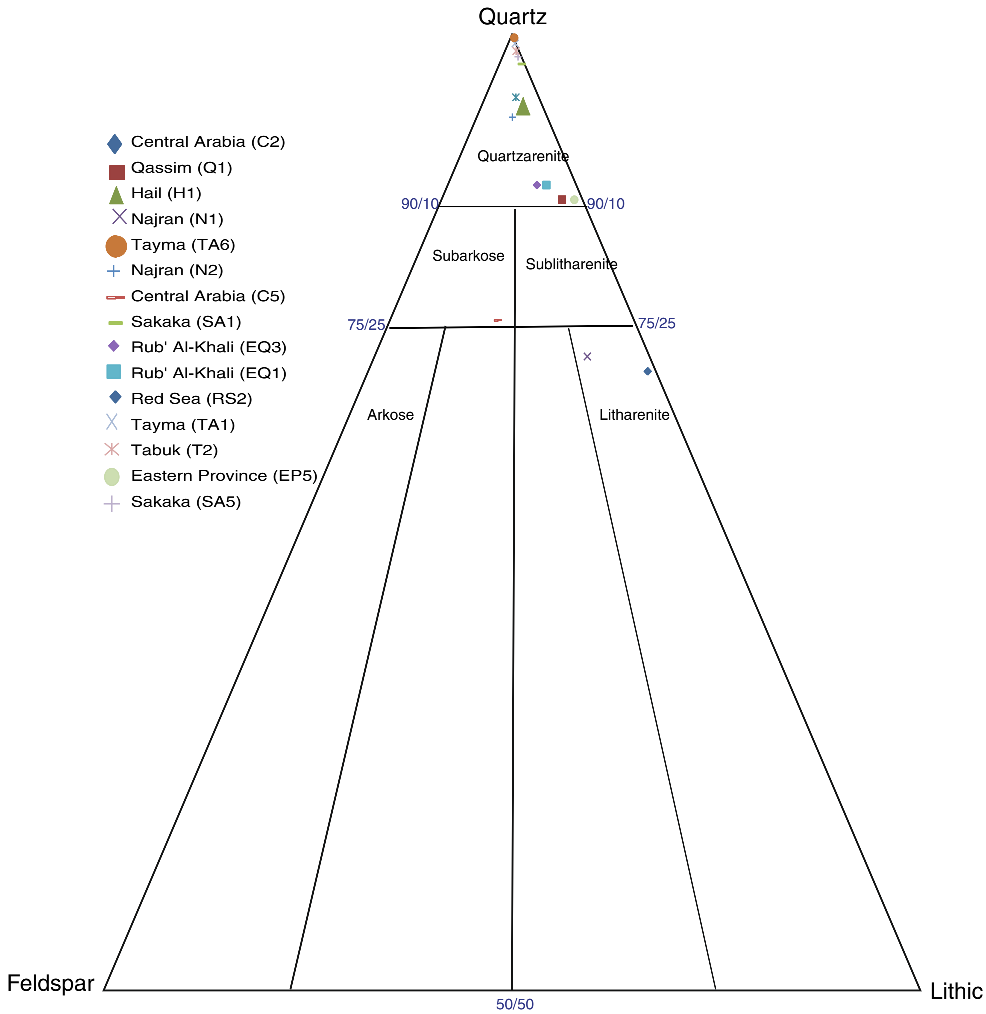

Fig. 4 QFR triangular classification plot (Folk 1974) of dune sands from ten locations in Saudi Arabia

Samples and analytical methods

The methods of study of sand dunes included both field work and laboratory sedimentological analyses. Sixty-seven sediment samples representing eolian sand dunes from 10 locations were collected. All samples were dry-sieved (Ingram 1971) to perform a granulometric analysis of grain textures. All samples were subjected to a grain roundness study using a binocular microscope. Sixteen samples were selected for bulk mineralogy analysis using powder X-ray diffractometer (XRD) analysis and petrographic examination. Before XRD analysis, samples were crushed to produce a powder, and then, the powder was loaded into an aluminum cavity holder and then mounted. Ni-filtered Cu radiation was used at a setting of 40 kV, and a scan was performed for 2-theta values from 2 up to 60°. The absolute peak area under the characteristic lattice spacing of the identified minerals was used as a measure of the relative abundance of minerals in bulk samples.

Sixteen samples were selected for surface texture analysis via a scanning electron microscope (SEM); an EDS unit was attached for elemental analysis. These samples were gold-coated and then mounted into a sample holder before being loaded into the SEM machine. The SEM was used to study the morphology of grain surfaces and to identify materials adhered to the surface of sand grains or within pits. Additionally, 16 samples were also selected for quantitative geochemical analysis to obtain major oxides, trace elements, and rare earth elements using ICP-MS technique.

Landsat satellite images with 30-m resolution were used to study the morphology of sand dunes. The images were enhanced using ENVI software making them useful to study of the morphology of the sand dune.

Results

Geomorphology

Sand dunes in Saudi Arabia occur as sand ridges extending from the Rub' Al-Khali Desert in the south and southeast to the An Nafud Desert in the north. These sand ridges form sand seas that reflect the direction of eolian sand movement during the Quaternary period (Shamall wind) (Edgell 2006) (Fig. 2). The sand ridges are controlled by rock escarpments and the direction of the paleowind. The geomorphology of sand ridges were studied using Landsat satellite images with 30-m resolution. In the An Nafud Desert (Hail, Tayma, Tabuk, and Sakaka locations), the sand dune ridges are linear with an E–W orientation northeast of the Hail area (Fig. 3a). These sand ridges extend southwards and connect to the Dahna Desert, where sand ridges change their orientation to NW–SE (Fig. 3b) and then N–S in the southern part of the Dahna Desert. In the Dahna Desert, the sand ridges extend southwards adjacent to the sedimentary rock escarpments, until the Najran area where it is connected by western part of Rub' Al-Khali desert and their orientation becomes NE–SW (Fig. 3c). In the Eastern Provinces, the sand ridges have an NE–SW orientation (Fig. 3d).

Climate and sedimentological factors controlled the accumulation of sands into sand dunes of particular shapes (Kenneth and Haim 2009). For example, parabolic sand dunes formed based on the accumulation of sand related to vegetation. This type of sand dune occurs in the An Nafud Desert at the Hail, Sakaka, and Tayama locations (Fig. 3e). However, other types of sand dunes, such as barchans, transverse, star, vegetated linear dunes, and dome dunes, were formed by the accumulation of sand based on bed roughness changes or aerodynamic fluctuation. These types of sand dunes also occur in Saudi Arabia. Unvegetated linear sand dunes occur in the Dahna Desert in central Arabia and the Rub' Al-Khali Desert. Dome dunes are recorded in central Arabia and occur between basement rocks and sedimentary rock outcrops such as those near Al-Muzahamiah town (Fig. 3f). Star dunes are the most dominant dune type in the Rub' Al-Khali and Dahna Deserts in central Arabia (Fig. 3g). These types of sand dunes occur within the sand ridges in these deserts, indicating that more than one direction of wind contributed to formation of the dunes. Barchan dunes characterize the sand dunes in the NW part of Rub' Al-Khali desert (Fig. 3h). Transverse sand dunes have been observed in many places, especially at the Al-Lidam area in the Eastern Province (Fig. 3d).

Sedimentology

Grain composition and classification

A petrographic analysis of the sand dunes was conducted for representative sand dunes from the different locations. Petrographic ternary QFL classification (Folk 1974) shows that the sand dunes from nonbasement-related areas are classified as quartz arenites, whereas the basement-related dunes from Najran (N1), central Arabia (C5), and the Red Sea are classified as subarkose to litharenite (Fig. 4).

Grain size distribution

The mean grain size distributions of all studied dunes are presented in histograms (Fig. 5). Sand dunes from the Red Sea, Sakaka, and the Eastern Province showed a unimodal distribution with a mean grain size in the fine modal class. However, the sand dunes from the Hail and Tayma areas exhibited unimodal distribution with mean grain size in the coarse modal class. Unimodal distribution with mean grain size from the medium modal class characterized dune sands from the Rub' Al-Khali, Tabuk, and central Arabia locations. Sand dunes from the Najran and Qassim locations showed no modal distribution.

Grain size parameters

The average values for all grain size parameters (mean, sorting, skewness, and kurtosis) of eolian sand dunes in Saudi Arabia are shown in Table 1. The average mean grain size covers three groups: fine, medium, and coarse. Sand dunes

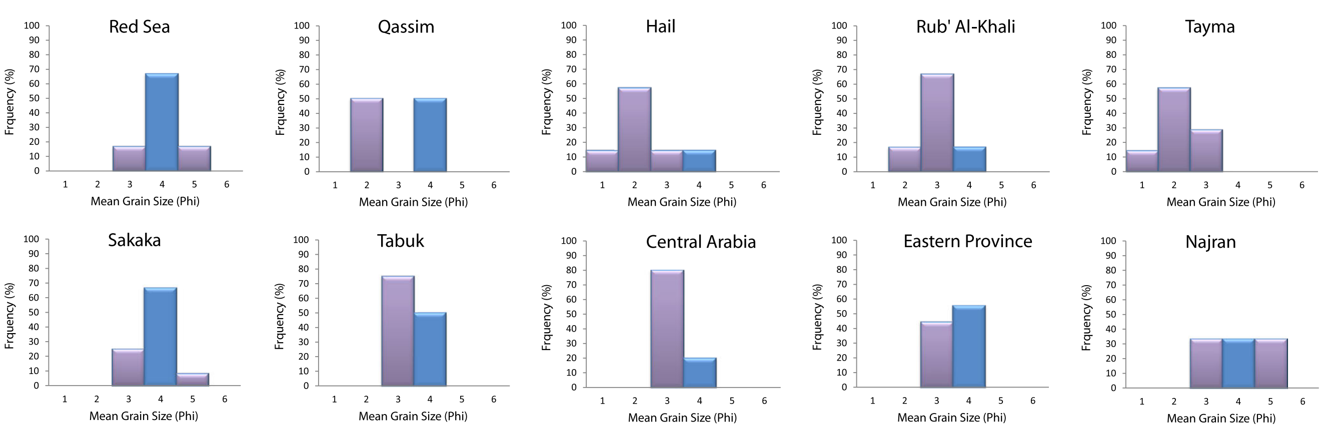

Fig. 5 Distribution histograms of mean grain size of dunes sands from ten locations in Saudi Arabia

Table 1 Statistical size parameters of dune sands from ten locations in Saudi Arabia

Location	Number of samples	Statistical size parameters (Phi)			
		Mean	Sorting	Skewness	Kurtosis
Central Arabia	5	1.710	0.880	−0.002	1.080
Eastern Province	9	1.999	0.740	−0.002	0.960
Rub' Al-Khali	12	1.460	0.863	0.131	0.936
Hail	7	0.861	0.767	0.098	0.960
Najran	3	2.433	0.740	0.074	4.063
Qassim	2	1.475	0.810	−0.003	1.115
Red Sea	6	2.513	1.008	0.112	0.997
Sakaka	12	2.290	0.802	0.001	1.014
Tabuk	4	1.735	0.738	0.015	1.004
Tayma	7	0.746	0.846	0.140	0.972

from the Hail and Tayma areas (An Nafud Desert) showed coarse mean grain size. On the other hand, the sand dunes from central Arabia, Rub' Al-Khali, Qassim, Tabuk, and the Eastern Province are characterized by a medium mean grain size. The sand dunes from Najran, the Red Sea, and Sakaka showed fine mean grain size. All the sands from studied locations are moderate to moderately well sorted, except sands from the Red Sea are poorly sorted. Sand dunes in all locations showed near symmetrical skewness, except those from the Red Sea, Rub' Al-Khali, and Tayma locations, which displayed a fine skewness. Moreover, all sand dunes were identified as mesokurtic, except those sand dunes at Najran and Qassim, which were leptokurtic.

Roundness

Two sand dune groups were identified based on grain roundness. The first group includes the sand dunes from the Red Sea, Qassim, central Arabia, and the Eastern Province. These dunes are characterized by subangular sand grains (Table 2). Moreover, the Red Sea sand dunes grains are more angular than those from other locations. The second group included sand dunes from the Rub' Al-Khali, Tayama, Sakaka, Najran, Hail, and Tabuk locations, which are characterized by subrounded sand grains (Table 2). Rub' Al-Khali and Najran sand dunes showed more rounded sand grains than those from the Tayma, Sakaka, Hail, and Tabuk locations.

Mineralogy

Bulk mineralogy for the 16 representative sand dunes was obtained using a powder XRD. The mineralogical composition of the sands consists mainly of quartz, feldspars, and calcite. The most dominant mineral in all studied locations is quartz (Fig. 6a). In some areas, feldspars and calcite occur as significant minerals. Dune sands from Hail, Tabuk, Tayma, Sakaka, and Rub' Al-Khali and nonbasement-related dune sands in Najran (N2) location (western part of Rub' Al-Khali desert) are entirely composed of quartz (Fig. 6a). Traces of calcite are found in samples from Sakaka and Rub' Al-Khali (Fig. 6b).

Quartz dominates in sand dunes from coastal Arabia, with a significant amount (<10 %) of calcite and low concentration of feldspars (albite) (Fig. 6b). The Qassim and nonbasement-related sand dunes in central Arabia showed feldspars (<10 %) as the subordinate minerals (Fig. 6c, d). Dune sands from the Red Sea, Najran (N1), and central Arabia (C5) (basement-related) were composed of quartz and a significant amount of feldspars (>10 %) (Fig. 6e). Using Folk's classification (QFL ternary plot) (Folk 1974), sand from nonbasement-related dunes were classified as quartz arenite, while basement-related dune sands from Najran (N1), central Arabia (C5), and the Red Sea were classified as subarkose to Litharenite (Fig. 4).

Grain surface microtexture

The SEM-EDS analyses of the surface morphology of sand grains from different dunes showed both mechanical and

Table 2 Relative frequency percentage of grains roundness

Location	Rounded	Subrounded	Subangular	Angular
Red Sea	3.7	7.4	74.1	14.8
Rub' Al-Khali	25.0	50.0	18.8	6.3
Najran	25.0	60.0	10.0	5.0
Qassim	6.7	16.7	66.7	10.0
Central Arabia	4.0	20.0	48.0	28.0
Hail	4.2	66.7	25.0	4.2
Tayma	5.0	64.0	25.0	4.2
Sakaka	10.0	60.0	25.0	5.0
Tabuk	6.3	62.5	25.0	6.3
Eastern Province	5.6	27.8	55.6	11.1

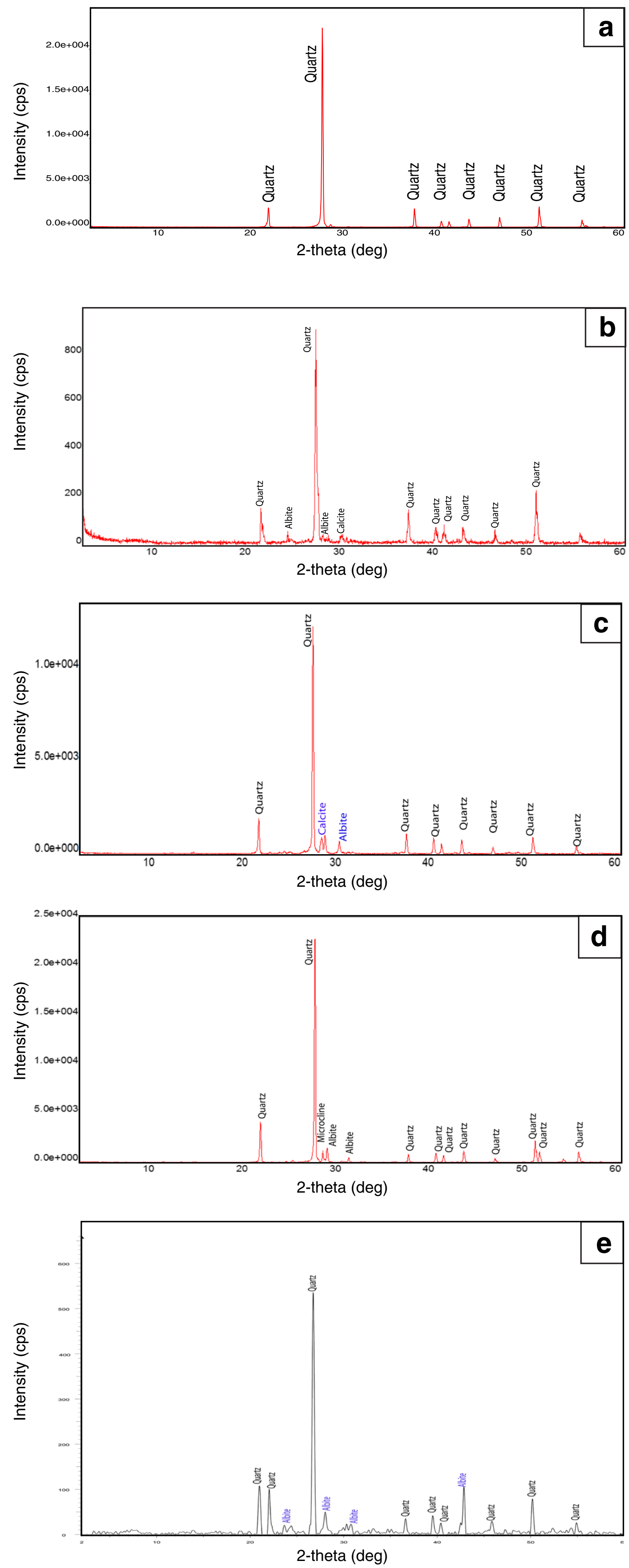

Fig. 6 XRD charts show the mineral composition of sand dunes. **a** Mainly quartz of dune sands from Tayma area. **b** Quartz, feldspar (albite), and trace of calcite of dune sand from Rub' Al-Khali. **c** Quartz, calcite, and feldspar (<10 %) of dune sands from Arabian Gulf coast. **d** Mainly quartz with feldspar (<10 %) of dune sands from central Arabia. **e** Quartz and feldspar (>10 %) of dune sands from the basement-related sand dunes, Najran area

chemical microtexture features (Table 3). Features due to mechanical weathering include upturned plates, mechanical impact pits, conchoidal fractures, irregular, and randomly oriented V-shaped patterns and meandering ridges. Most of the sand grains from all locations showed various types of chemical features, such as solution bits, and hacksaw, regular, and oriented V-shaped patterns.

Mechanical features noted on sand grains included abundant pits on the surface of quartz grains in dune sands from the Sakaka area (Fig. 7a). Upturned plates were also recorded on sand grains from the Najran, central Arabia, Qassim, and Sakaka locations (Fig. 7b). The surface of sand grains from Najran and Tayma showed conchoidal fractures (Fig. 7b, c). Meandering ridges were observed on grain surfaces of dune sands from the Red Sea (Fig. 7d). Randomly oriented V-shaped patterns with irregular outlines as the result of mechanical processes were observed on grains from Hail and Tayma dunes (Fig. 7e).

An SEM examination of the sand grains revealed some chemical features on grain surfaces. These features included solution pits, hacksaw termination, and regular and oriented patterns of V-shaped. Solution pits are dominant on the surfaces of the sand grains from Sakaka, Tayma, and Tabuk (Fig. 7f). V-shaped patterns with regular outlines and oriented patterns as a result of chemical processes are noted on the surfaces of sand grains from the Arabian Gulf coastal plain sand dunes (Fig. 7g). Hacksaw terminations were observed on the surface of sand grains from central Arabia (Fig. 7h).

Adhering materials located within pits and other impact regions on the surface of sand grains are produced by mechanical and chemical processes. These materials vary in composition; their mineralogical composition includes quartz, wollastonite, garnet, aluminum silicate minerals (kyanite, andalusite, and sillimanite), olivine (fayalite), and microcline.

Adhering quartz grains are observed in all samples from different areas (Fig. 8a). In addition, adhering microcline grains occurred on the surface of sand grains from the Hail area in the northern part of Saudi Arabia (Fig. 8b). Adhering garnet grains are observed on the surfaces of sand grains from the Najran and Sakaka locations, along with almandine in Najran sand grains (Fig. 8c) and pyrope type of garnet occurs as adhering material in Sakaka sand grains (Fig. 8d). Dune sands from the Eastern Province, Rub' Al-Khali, the Red Sea, and Tayma locations are characterized by the presence of wollastonite-adhering minerals (Fig. 8e). Aluminum silicate minerals (kyanize, andalusite, and sillimanite) were also observed adhering to grains in dune sands from the Eastern Province, Hail, Qassim, Tabuk, and the Red Sea locations (Fig. 8f). An olivine mineral (fayalite?) exists solely as adhering grains in sands grain from sand dunes located NE of Riyadh in the Dahna Desert on a site near the Riyadh Dammam Road (Fig. 8g).

Geochemical analysis

Geochemical analyses were conducted to determine the concentrations of the major, trace, and rare earth elements in 16 samples representing the sand dunes from different areas of Saudi Arabia (Table 4).

Table 3 Table shows surface features of sand grains from ten locations of sand dunes in Saudi Arabia (P=present)

Features	Locations									
	Red sea	Central Arabia	Najran	Hail	Tayma	Tabuk	Sakaka	Qassim	Eastern Provinces	Rub' Al-Khali
Mechanical origin										
Pits							P			
Conchoidal fractures			p		p					
Straight steps				p						
Arcuate steps										
Upturned plates		p	p				P	p		p
Imbricated grinding features		p				p				
Meandering ridges	p				p					
Straight scratches										
Curved scratches										
Subangular outline	p	p				p				
Rounded outline			p	p	p		P	p	p	p
V-shaped patterns				p					p	
Mechanical/chemical origin										
Adhering particles	p	p	p	p	p	p	P	p	p	p
Chemical origin										
Solution pits				p			P			

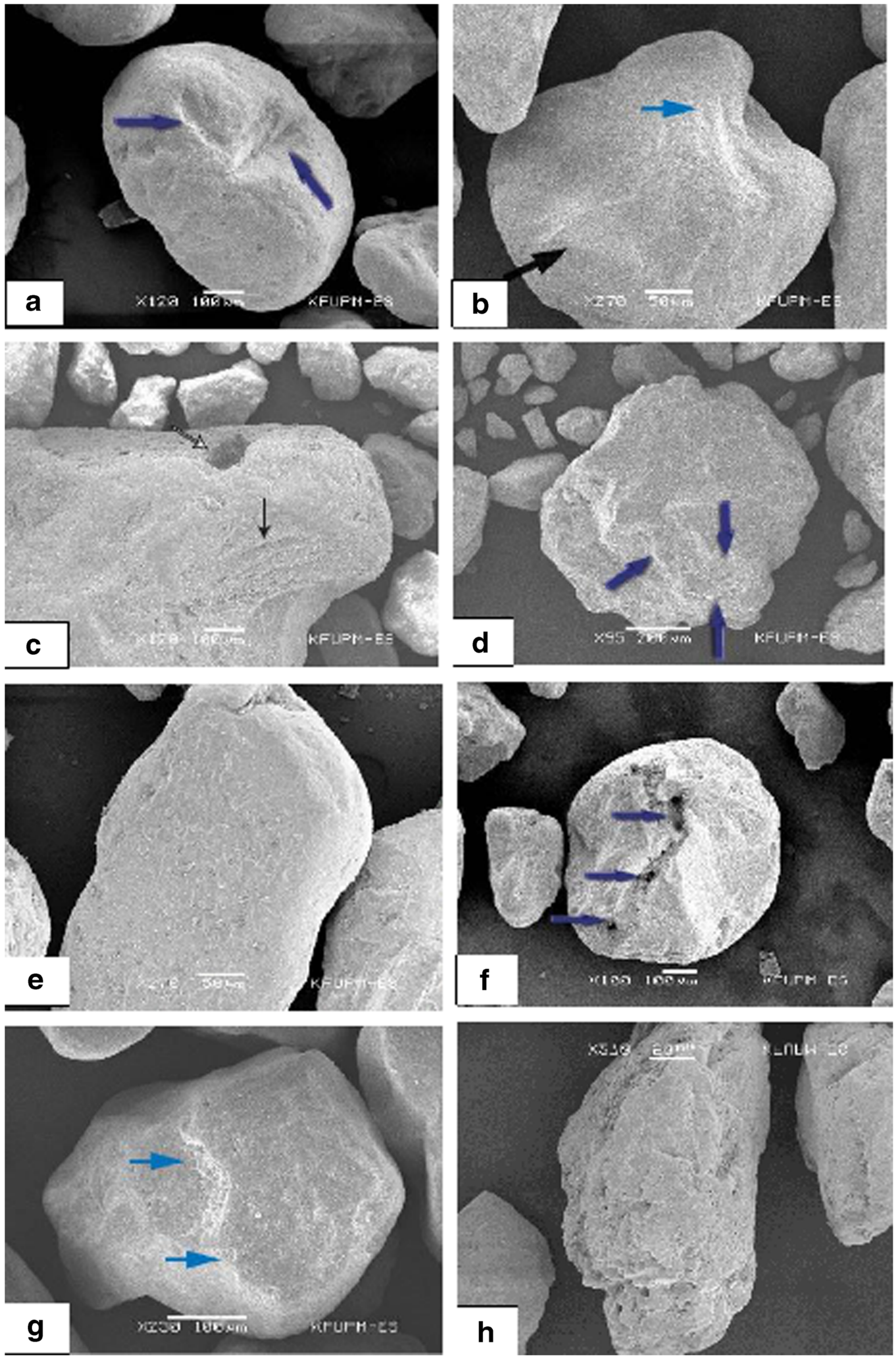

Fig. 7 SEM microphotograph of sand dune grains showing **a** large pits on the surface of Quartz grain (Sakaka area), **b** upturned plate (*black arrow*) and conchoidal fractures (*dark arrow*) (Najran area), **c** conchoidal fractures (*black arrow*) and solution pit (*white arrow*) (Tayma area), **d** Meandering Ridges (*arrows*), Red Sea area, **e** V-shaped pattern with irregular shape and different orientation on sand grains (Hail area), **f** solution pits in surface of quartz grain (Sakaka area), **g** V-shaped pattern with regular outlines and oriented patterns, Arabian Gulf coastal dunes and **h** hacksaw termination of sand grains, central Saudi Arabia

Distribution of elements

Sixteen samples from different sand dunes from 10 locations were analyzed to determine the concentration of major oxides, as well as trace and rare elements (Table 4). Comparison of the distribution of major oxides allowed as to identify two groups of sand dunes (Fig. 9). The first group includes sand dunes from the northern part of Rub' Al-Khali, Qassim, Hail, the Eastern Province, Sakaka, Tabuk, Tayma, and central Arabia. Sand dunes at the aforementioned locations are characterized by a high percentage of SiO_2 and a very low percentage of feldspars (Fig. 9). The second group includes sand dunes from

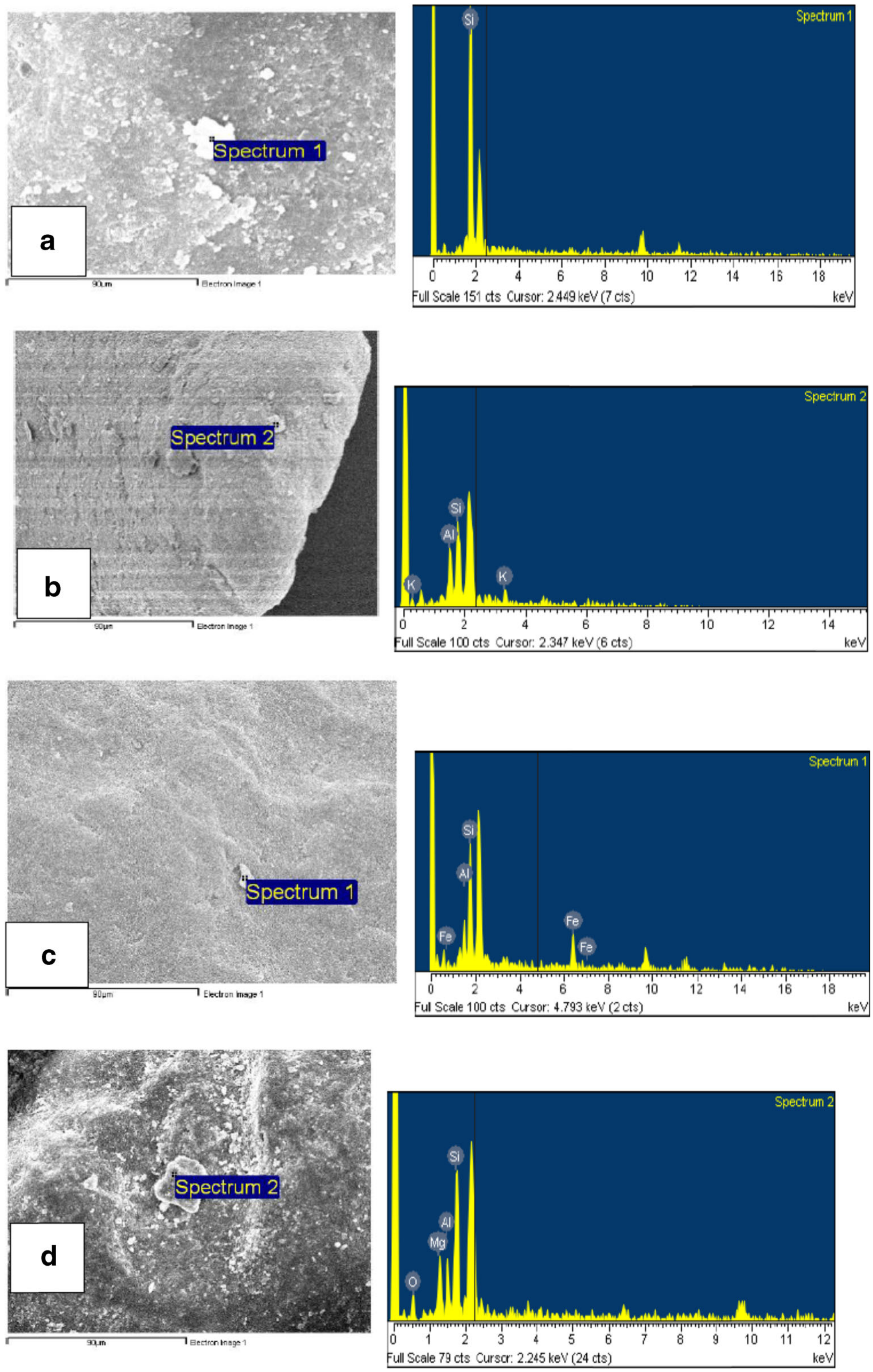

Fig. 8 SEM-EDS analysis of sand dune grains showing adhering material on the surface of sand grains: **a** adhering quartz grain, **b** adhering microcline grain, **c** adhering garnet (almandine) grain, **d** adhering garnet (pyrope) grain, **e** adhering wollastonite grain, **f** adhering aluminum silicate minerals grain, and **g** adhering olivine mineral (fayalite) grain

the Red Sea, Najran (N1), and central Arabia (C5), and all are basement-related sand dunes. These sand dunes are characterized by a high percentage of quartz with a significant amount of feldspars (Fig. 9).

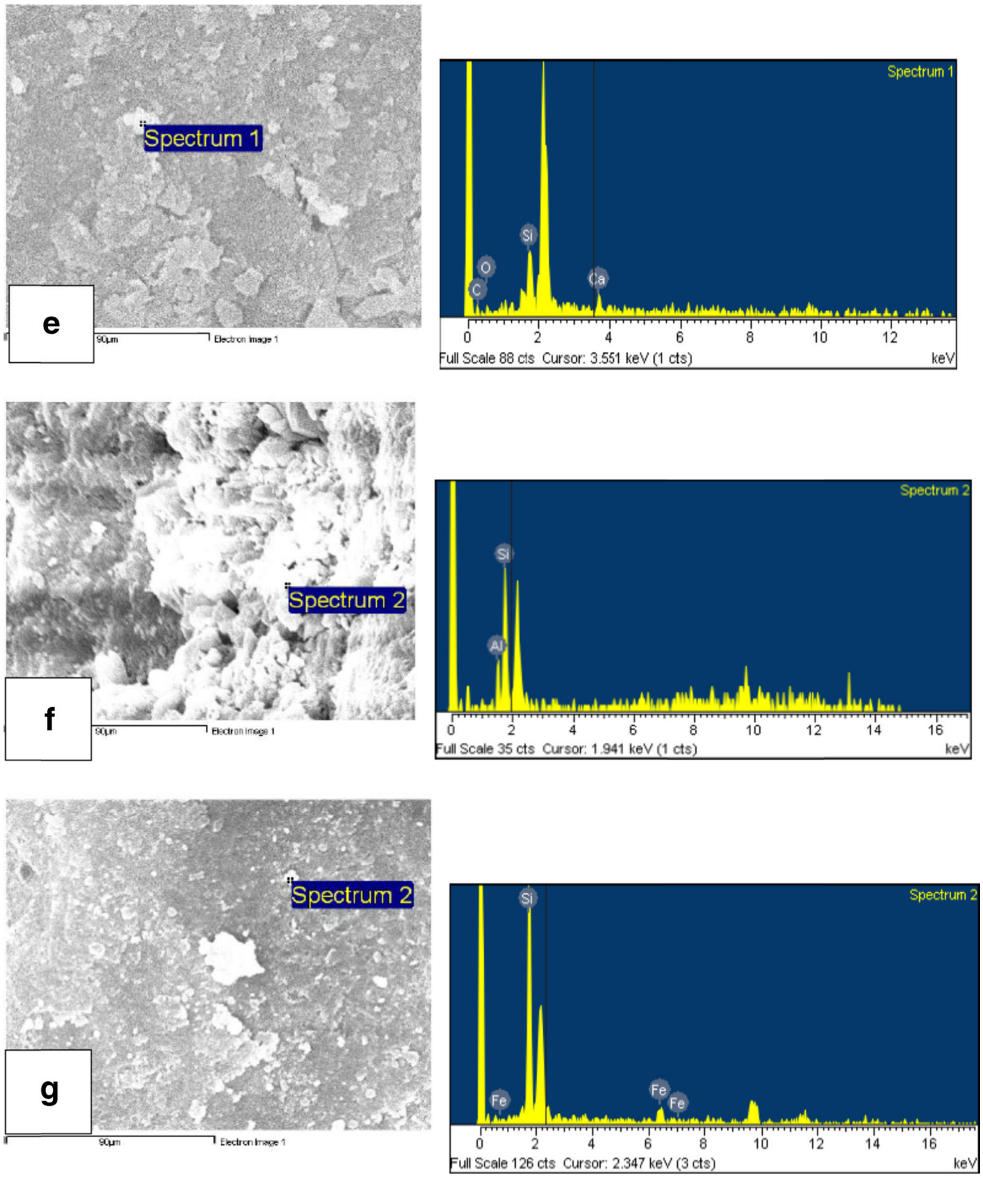

Fig. 8 (continued)

The distribution of major elements (Fig. 10) shows that sand dunes from Sakaka and central Arabia (C5) (basement-related sand dunes, Al-Dawadmi) are similar in their carbon and sulfur contents, which are 97 % carbon and 3 % sulfur, respectively. The sand dunes from Hail, central Arabia (C2), Najran (N1), Najran (N2) (basement-and nonbasement-related sand dunes), the Eastern Province, Tabuk, Rub' Al-khali, the Red Sea, and Qassim are characterized by carbon concentration of 90 % in average and sulfur of about 10 % (Fig. 10). Furthermore, the sand dunes from the Tayma location contain the lowest amount of carbon of 84 % and the highest concentration of sulfur, 16 %, of these locations (Fig. 10).

The distribution of trace earth elements in sand dunes showed that the most dominant trace earth elements are Ba, Cr, Rb, Sr, V, Zr, Ni, and Zn. Trace element concentrations in sand dunes from the Red Sea, Najran (N1), and central Arabia (C5) are similar. The concentrations of the trace elements in these dunes is high (Fig. 11), except Zr, which is less dominant in the Red Sea sand dunes than the other areas. In contrast, Hail and Qassim sand dunes show the highest concentration of Zr (Fig. 11). The sand dunes from Tayma, Rub' Al-Khali, Hail, Sakaka, Tabuk, central Arabia (C2) (nonbasement-related sand dunes), Najran (N2) (nonbasement-related sand dunes), Qassim, and the Eastern Province are characterized by less concentration of trace elements relative to the other locations (Fig. 11).

The distribution of rare earth elements was similar among sand dunes from the Red Sea, Najran (N1), and central Arabia (C5) (all basement-related sand dunes), with relatively high concentrations, in parts per million values (Fig. 12). However, the remaining locations have lower concentrations of rare earth elements than the previous group (Fig. 12). Sand dunes

Table 4 Major, trace, and rare earth elements concentration of dune sands from ten locations in Saudi Arabia

Sample	SiO_2 (%)	Al_2O_3 (%)	Fe_2O_3 (%)	CaO (%)	MgO (%)	Na_2O (%)	K_2O (%)	Cr_2O_3 (%)	TiO_2 (%)	MnO (%)	P_2O_5 (%)	SrO (%)	BaO (%)	C (%)	S (%)	Ba (ppm)
RS2	69.5	10.15	5.4	4.61	2.01	2.42	1.22	0.01	1.48	0.09	0.21	0.05	0.03	0.36	0.04	300
C2	93	3.53	.074	.073	0.34	0.8	0.91	0.01	0.15	0.01	0.02	0.02	0.02	0.12	0.01	240
Q1	94.1	2.35	0.8	0.36	0.25	0.35	0.65	0.01	0.18	0.01	0.02	0.01	0.02	0.12	0.01	181
H1	96.9	1.7	0.59	0.21	0.19	0.09	0.085	0.01	0.1	0.02	0.03	0.01	0.03	0.09	0.01	223
N1	73.9	10.2	4.54	3.44	1.82	2.14	1.53	0.02	0.6	0.07	0.14	0.03	0.04	0.26	0.03	360
TA6	99.1	0.19	0.32	0.14	0.03	0.02	0.03	0.02	0.02	<0.01	<0.01	<0.01	<0.01	0.05	0.01	18.2
N2	93.1	2.27	0.74	0.84	0.25	0.41	0.64	0.01	0.17	0.01	0.02	0.01	0.02	0.11	0.01	139.5
C5	76.2	10.8	2.34	2.25	1.1	2.98	1.91	0.01	0.62	0.05	0.07	0.03	0.05	0.28	0.01	458
SA1	94	1.36	0.66	0.96	0.37	0.03	0.55	0.01	0.13	0.01	0.03	<0.01	0.02	0.32	<0.01	181
EQ3	90.8	3.04	0.69	2.21	0.42	0.51	1.28	0.02	0.13	0.01	0.01	0.01	0.04	0.45	0.02	279
EQ1	93.4	2.05	0.55	1.67	0.25	0.26	0.97	0.02	0.07	0.01	0.02	0.01	0.02	0.35	0.07	207
RS7	72.4	11.8	3.22	3.41	1.17	2.64	2.8	0.01	0.63	0.06	0.09	0.05	0.09	0.18	0.02	720
TA1	98.7	0.43	0.38	0.04	0.05	0.06	0.05	0.02	0.03	<0.01	<0.01	<0.01	<0.01	0.05	<0.01	21
T2	95.5	1.43	0.85	0.33	0.21	0.1	0.23	0.01	0.13	0.01	0.04	0.01	0.01	0.09	<0.01	42
EP5	94	1.66	0.58	0.18	0.12	0.26	0.56	0.01	0.08	0.01	0.02	<0.01	0.01	0.07	<0.01	59.2
SA5	95.3	1.33	0.54	0.7	0.2	0.1	0.66	0.01	0.1	0.01	0.04	<0.01	0.02	0.19	<0.01	167

Sample	Ce (ppm)	Cr (ppm)	Cs (ppm)	Dy (ppm)	Er (ppm)	Eu (ppm)	Ga (ppm)	Gd (ppm)	Hf (ppm)	Ho (ppm)	La (ppm)	Lu (ppm)	Nb (ppm)	Nd (ppm)	Pr (ppm)
RS2	36.2	110	0.68	5.66	3.52	1.49	14.2	5.13	3.8	1.21	16.6	0.05	10.8	20.5	4.85
C2	17.1	60	0.6	1.21	0.85	0.36	5.1	1.23	4	0.21	8.6	0.1	2.4	7.3	1.91
Q1	27.6	100	0.48	1.4	0.85	0.41	3.4	1.67	5.4	0.3	12.9	0.13	3.4	11	2.98
H1	24	50	0.33	0.99	0.67	0.3	2.3	1.05	9	0.2	11.3	0.14	1.8	9.5	2.55
N1	30.2	120	0.9	3.21	1.84	0.92	14.3	3.43	5.1	0.6	13.8	0.3	5.7	16.1	3.75
TA6	6.5	140	0.02	0.43	0.24	0.07	0.4	0.5	1.4	0.09	3	0.04	0.5	2.6	0.71
N2	10.4	100	0.31	0.82	0.55	0.26	2.9	0.87	4.3	0.19	5.1	0.08	1.8	5.1	1.31
C5	26.6	70	1.38	3.64	2.02	0.79	12.4	3.41	7.8	0.74	12.5	0.28	7.7	13.7	3.35
SA1	20	50	0.29	0.95	0.6	0.37	2.1	1.33	3.9	0.16	9.8	0.09	2.5	8.6	2.26
EQ3	87	160	0.52	0.73	0.54	0.19	3.9	0.73	4.9	0.13	4.6	0.07	1.7	4.3	1.1
EQ1	5.9	150	0.37	0.45	0.38	0.13	2.2	0.38	1.9	0.1	3.4	0.06	1.2	3.2	0.75
RS7	36.4	90	0.43	2.65	1.38	0.99	13	3.22	4.4	0.46	17.5	0.18	4.4	18.5	4.78
TA1	10.9	140	0.21	0.64	0.33	0.12	0.7	0.7	2.5	0.12	5.3	0.04	0.6	4.5	1.18
T2	13.7	40	0.32	1.01	0.51	0.21	1.8	0.95	4.9	0.22	6.7	0.08	2.4	5.8	1.53
EP5	11.2	40	0.34	0.97	0.58	0.22	2.5	10.2	4.8	0.16	6.1	0.08	2	5.7	1.48
SA5	16	50	0.27	0.97	0.64	0.24	1.8	1.04	4.1	0.18	7.9	0.09	1.9	6.9	1.76

Sample	Rb (ppm)	Sm (ppm)	Sn (ppm)	Sr (ppm)	Ta (ppm)	Tb (ppm)	Th (ppm)	Tl (ppm)	Tm (ppm)	U (ppm)	V (ppm)	W (ppm)	Y (ppm)	Yb (ppm)	Zr (ppm)	As (ppm)
RS2	26.3	4.98	1	394	0.8	0.87	2.28	<0.5	0.5	1.08	143	1	34.1	3.22	143	8.9
C2	25.6	1.37	1	139.5	0.2	0.17	2.24	<0.5	0.12	0.77	20	<1	6.8	0.8	155	0.7
Q1	17.7	2.37	1	80.1	0.2	0.24	4.42	<0.5	0.14	0.97	16	1	8	0.76	223	1
H1	19.7	1.69	<1	54	0.1	0.14	1.94	<0.5	0.1	0.99	10	1	5.3	0.76	367	0.4
N1	37.4	3.42	1	251	0.4	0.5	3.34	<0.5	0.28	1.13	100	1	17.3	2.02	209	5.4
TA6	0.6	0.54	<1	15.3	<0.1	0.06	1.39	<0.5	0.05	0.47	<5	1	2.3	0.22	51	0.2
N2	13.7	0.91	<1	67.8	0.1	0.14	1.07	<0.05	0.08	0.41	15	1	4.6	0.65	182	0.3
C5	54.7	3.08	1	279	0.6	0.55	12.8	<0.5	0.28	2.8	55	1	20.2	1.83	329	4.2

Table 4 (continued)

Sample	Rb (ppm)	Sm (ppm)	Sn (ppm)	Sr (ppm)	Ta (ppm)	Tb (ppm)	Th (ppm)	Tl (ppm)	Tm (ppm)	U (ppm)	V (ppm)	W (ppm)	Y (ppm)	Yb (ppm)	Zr (ppm)	As (ppm)
SA1	15.9	1.39	<1	49.9	0.1	0.18	1.97	<0.5	0.09	0.63	13	1	5.1	0.45	157	0.8
EQ3	26.9	0.83	1	107	0.1	0.11	1.78	<0.5	0.08	0.49	11	1	4.3	0.51	204	1
EQ1	22	0.53	1	131	0.1	0.07	0.77	<0.5	0.06	0.34	9	1	2.9	0.39	75	0.6
RS7	51.4	3.46	1	370	0.3	0.45	3.1	<0.5	0.17	0.81	76	1	13.4	1.29	171	0.4
TA1	1.3	0.62	<1	22.5	<0.1	0.09	1.62	<0.5	0.03	0.4	<5	1	2.9	0.3	106	0.3
T2	6	1.1	<1	69.6	0.1	0.15	2.19	<0.5	0.08	0.63	10	1	5.2	0.58	191	0.6
EP5	13.8	1.23	1	30.6	0.1	0.14	1.54	<0.5	0.07	0.46	<5	1	5.2	0.58	193	0.3
SA5	16.2	1.12	<1	46.9	0.1	0.16	1.71	<0.5	0.1	0.63	8	1	5.3	0.61	158	0.5

Sample	Bi (ppm)	Hg (ppm)	Sb (ppm)	Se (ppm)	Te (ppm)	LOl (%)	Total (%)	Ag (ppm)	Cd (ppm)	Co (ppm)	Cu (ppm)	Li (ppm)	Mo (ppm)	Ni (ppm)	Pb (ppm)	Sc (ppm)	Zn (ppm)
RS2	0.05	0.008	0.14	0.4	0.02	2.89	100.07	<0.5	<0.5	14	18	10	<1	28	5	16	58
C2	0.03	<0.005	0.05	<0.2	0.01	0.96	101.24	<0.5	<0.5	2	4	<10	<1	7	7	2	9
Q1	0.02	0.007	0.09	<0.2	0.01	1.06	100.17	<0.5	<0.5	2	5	<10	<1	7	8	2	10
H1	0.02	0.005	<0.05	<0.2	<0.01	0.8	101.53	<0.5	<0.5	2	4	<10	<1	4	7	1	6
N1	0.05	0.011	0.21	0.5	0.02	2.73	101.2	<0.5	<0.5	11	17	10	<1	24	8	12	51
TA6	<0.01	<0.005	0.06	<0.2	<0.01	0.31	100.18	<0.5	<0.5	<1	5	<10	<1	4	4	<1	2
N2	0.01	<0.005	0.05	<0.2	<0.01	0.91	99.4	<0.5	<0.5	2	4	<10	<1	9	5	2	6
C5	0.05	0.006	0.11	0.3	0.02	2.22	100.83	<0.5	<0.5	6	10	10	<1	20	10	6	32
SA1	0.01	<0.005	<0.05	<0.2	0.01	1.86	99.99	<0.5	<0.5	2	2	<10	<1	6	8	1	4
EQ3	0.01	0.005	0.1	<0.2	0.01	2.6	101.77	<0.5	<0.5	2	4	<10	<1	9	5	1	6
EQ1	0.01	0.006	0.08	<0.2	0.01	2.05	101.35	<0.5	<0.5	1	4	<10	1	8	5	1	4
RS7	0.02	0.008	0.05	0.3	0.01	2.11	100.48	<0.5	<0.5	7	10	<10	<1	14	10	8	30
TA1	0.02	<0.005	0.06	<0.2	<0.01	0.64	100.4	<0.5	<0.5	1	5	<10	<1	4	15	1	4
T2	0.02	<0.005	0.05	<0.2	0.01	1.39	100.25	<0.5	<0.5	1	3	<10	<1	6	10	2	9
EP5	0.02	<0.005	<0.05	<0.2	<0.01	0.94	98.43	<0.5	<0.5	<1	2	<10	<1	5	5	1	8
SA5	0.01	<0.005	<0.05	<0.2	0.01	1	110.01	<0.5	<0.5	2	3	<10	<1	4	6	1	6

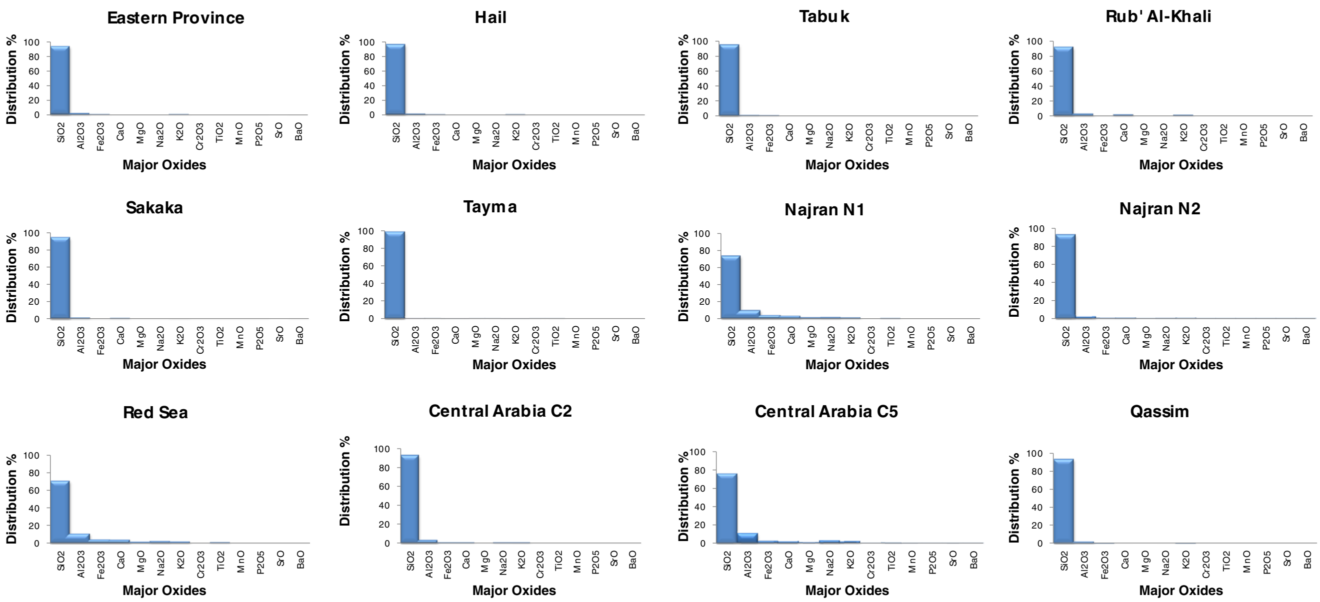

Fig. 9 Distribution of major oxides of dune sands from ten locations in Saudi Arabia

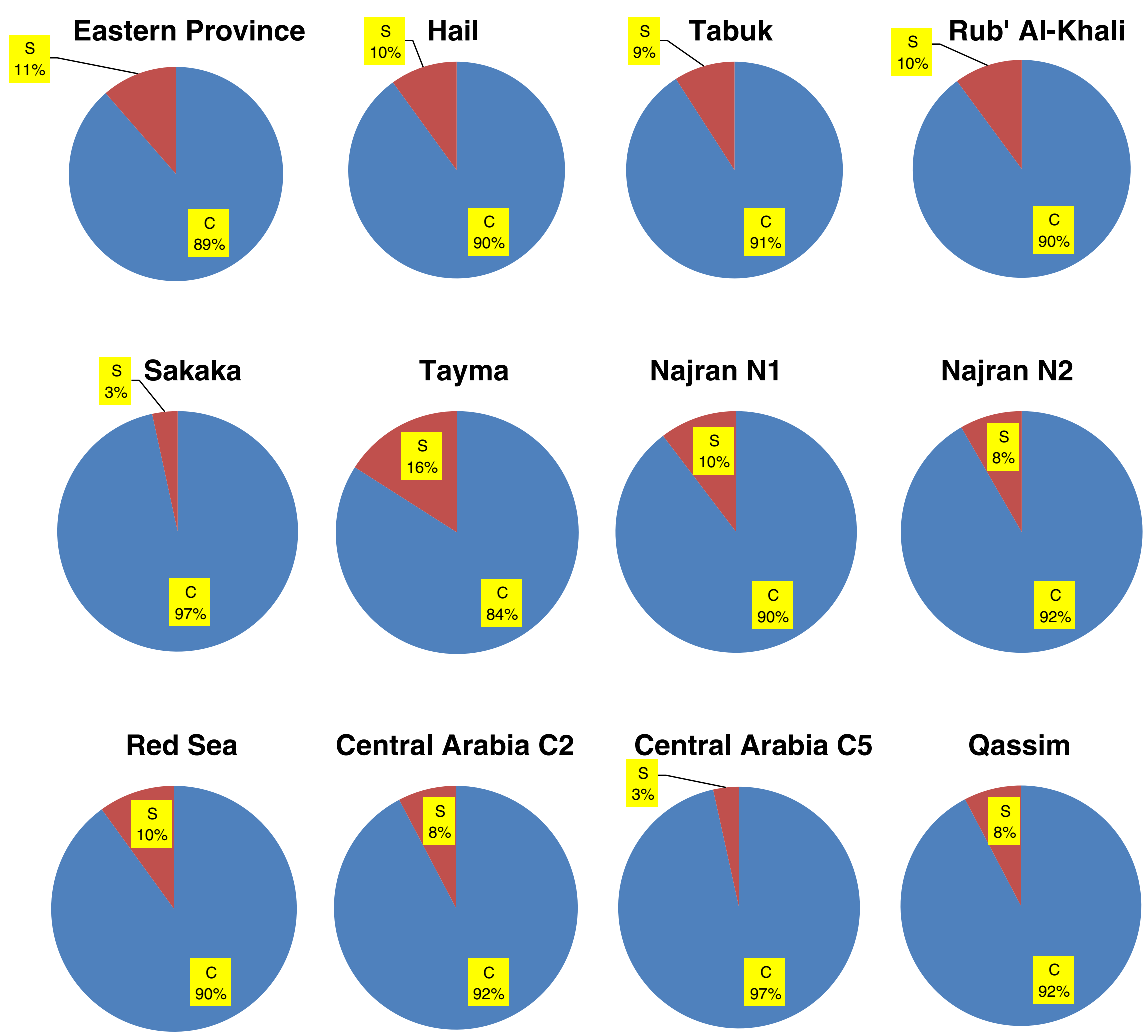

Fig. 10 Distribution of trace elements of dune sands from ten locations in Saudi Arabia

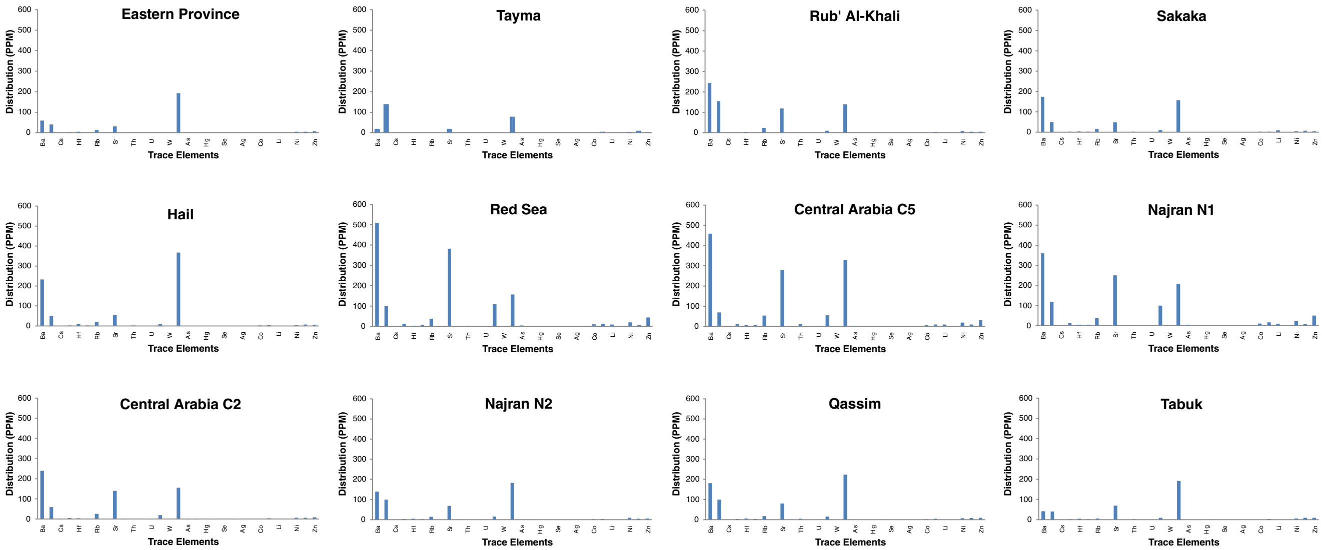

Fig. 11 Distribution of trace elements of dune sands from ten locations in Saudi Arabia

from the Qassim area contained some rare earth elements of the first group, such as Ce, La, Nd, Pr, and Sm. However, this location also contained rare earth elements of the second group (Fig. 12).

Geochemical classification

Based on the geochemical classification diagram of sand developed by Herron (1988), most of the dune sands from the studied locations were identified as quartz arenite (Fig. 13a). The only few exceptions are the sand dunes from Najran (N1), the Red Sea, and central Arabia (C5) (basement-related sand dunes), which are classified as subarkose, litharenite, and greywacke (Fig. 13a). An A–B diagram was plotted for sand dunes from all studied locations, where A=SiO_2 and B=K_2O+Na_2O+Al_2O_3 (Muhs 2004) to determine their mineralogical maturity. Sand dunes from most of studied locations have high mineralogical maturity. Those from Najran (N1), the Red Sea, and central Arabia (C5) (basement-related sand dunes) are the few that exhibit low mineralogical maturity (Fig. 13b). The sand dunes from the Tayma area exhibit the highest mineralogical maturity (Fig. 13b).

In the chondrite-normalized rare earth element (REE) diagram (Fig. 13c), the 10 studied locations of sand dunes show light REE (LREE) enrichment and heavy REE (HREE) depletion patterns.

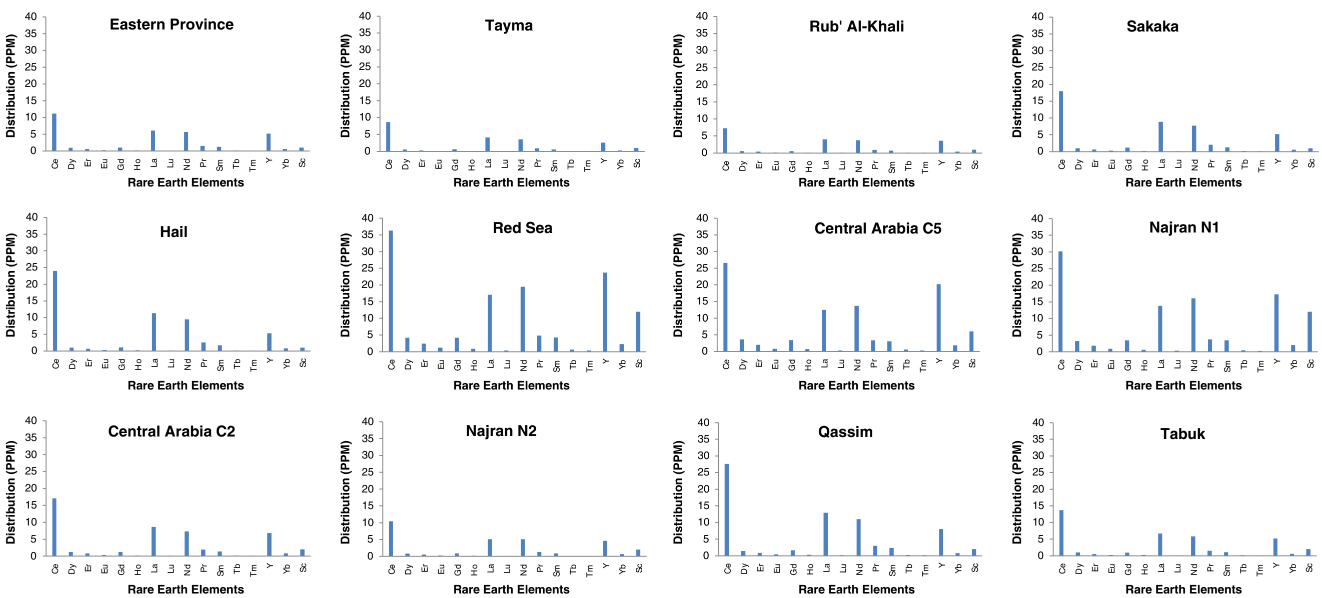

Fig. 12 Distribution of rare earth elements of dune sands from ten locations in Saudi Arabia

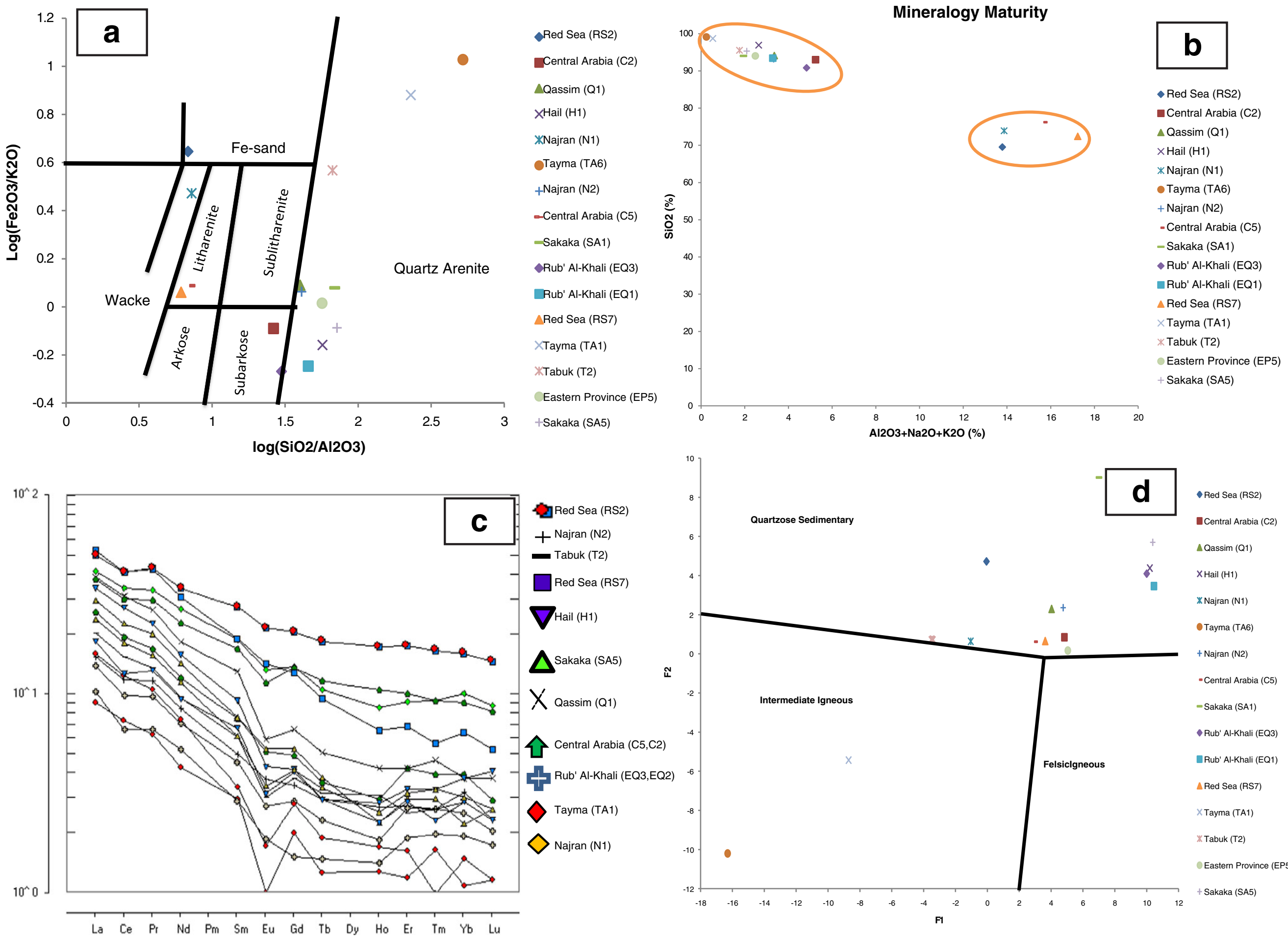

Fig. 13 **a** Geochemical classification of sandstone for dune sands from ten locations in Saudi Arabia using log Fe_2O_3/K O vs. log SiO/Al_2O_3 (after Herron 1988). **b** Discrimination diagram shows the mineralogy maturity of the studied dune sands (after Muhs 2004). **c** REE chondrite normalized diagram for the studied dune sands. **d** Major elements discrimination diagram for sedimentary provenance of the studied dune sands. **e** Major elements discrimination diagram of the studied dune sands shows the tectonic setting, (***C***) active continental margin and (***D***) Passive continental margins (after Bhatia 1983). **f** Major elements discrimination diagram of the studied dune sands shows the tectonic setting (after Bhatia 1983). **g** La–Th–Sc tectonic discrimination ternary: ***A*** oceanic island Arc, ***B*** continental island arc, ***C*** active continental margin, and ***D*** passive margin (after Bhatia and Crook 1986). **h** La/Yb vs. La/Th plot of the studied dune sands shows upper continental crust for the most locations and bulk continental for Sakaka and Tayma areas (*UC* upper continental crust, *TC* bulk continental crust, and *OC* average oceanic crust)

Provenance

Provenance of dune sands can be determined using the discriminant function diagram for provenance signatures of sandstone–mudstone suites using major element ratios (Roser and Korsch 1988). The two discriminant functions (Fs) are as follows: F_1=30.638 TiO_2/Al2O_3−12.541 Fe_2O_3 (total)/Al_2O_3+7.329 Mg/Al_2O_3+12.031 Na_2O/Al_2O_3+35.402 K_2O/Al_2O_3−6.382 and F_2=56.500 TiO_2/Al_2O_3−10.879 Fe_2O_3 (total)/Al_2O_3+30.875 Mg/Al_2O_3−5.404 Na_2O/Al_2O_3+11.112 K_2O/Al_2O_3−3.89). Based on the two discriminant functions, dune sands from all studied locations fell within the quartzose sedimentary dune provenance, except sand from the Tayma location, which occurred within the intermediate igneous provenance (Fig. 13d).

Tectonic setting

Major element geochemistry of the dune sands were plotted in discrimination diagrams to characterize dune tectonic settings, as proposed by Bhatia (1983). The first discrimination diagram was created by plotting MgO+Fe_2O_3 vs. Al_2O_3/SiO_2 (Fig. 13e), and the second one was developed by plotting K_2O/Na_2O vs. SiO_2/Al_2O_3 (Fig. 13f). These diagrams showed that most of sand dunes indicated passive continental margin tectonic setting. The basement-related sand dunes in the Red Sea, central Arabia (C5), and Najran (N1) locations, however, revealed active continental margins (Fig. 13e, f).

Trace elements geochemistry discrimination diagrams were also used to characterize sand dune tectonic settings (Bhatia and Crook 1986). The ternary plot of La–Th–Sc

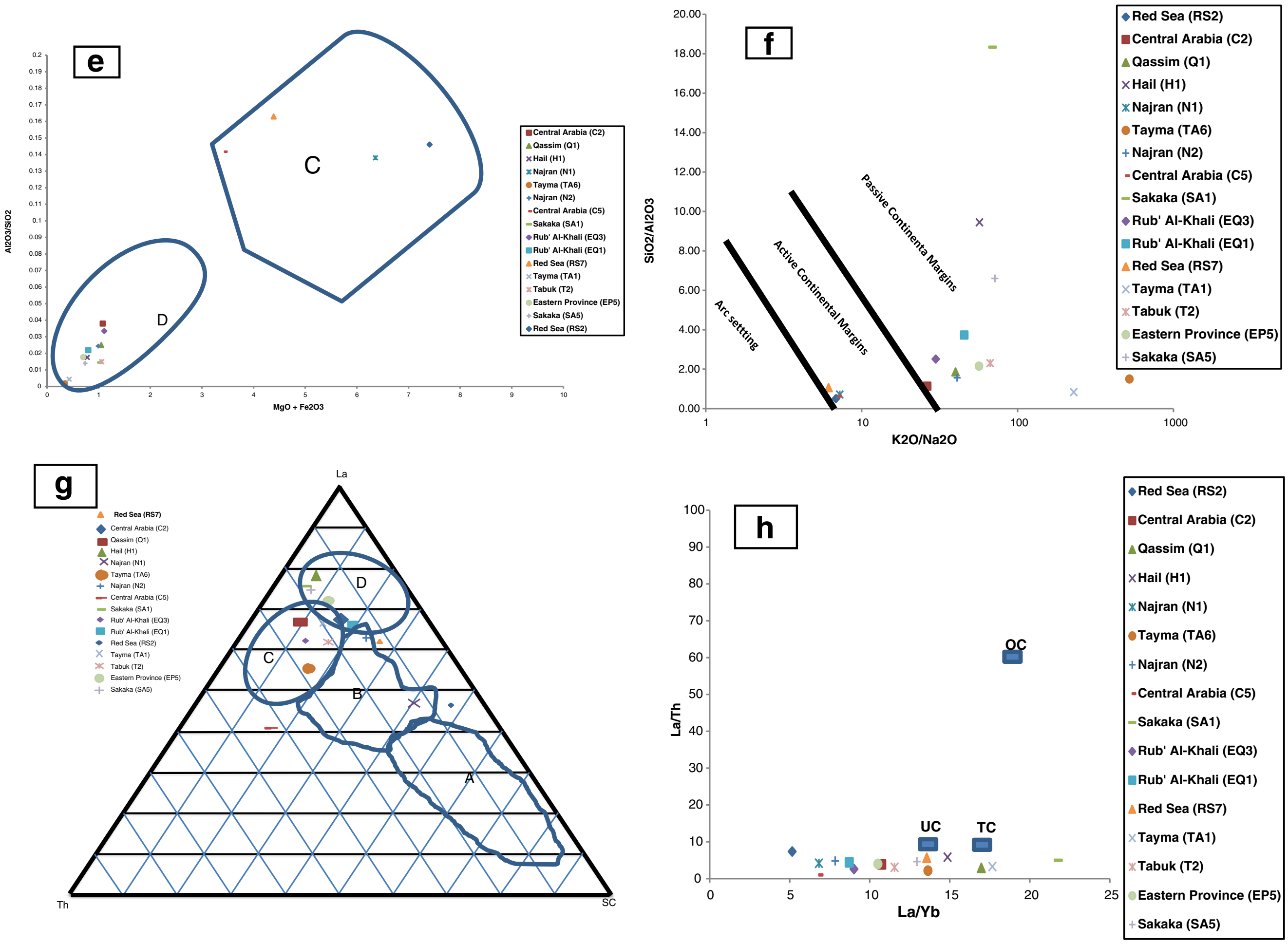

Fig. 13 (continued)

showed active continental margins (C) for Rub' Al-Khali and Tabuk sand dunes, continental island arcs (B) for nonbasement-related dunes in central Arabia (C2) and basement-related sand dunes in the Najran (N1) location, and passive continental margins for the remaining locations (Fig. 13g).

Furthermore, a discrimination diagram of the ratio of trace elements La/Yb and La/Th revealed that most of the sand dunes fit within an upper continental crust affinity except sand dunes from Sakaka and Tayma, which occurred within the bulk continental crust affinity (Fig. 13h).

Discussion and interpretations

Different orientations of sand dune ridges in the Rub' Al-Khali Desert in the south and the An Nafud Desert in the north reflect variations in paleowind directions during the Quaternary period. Moreover, the presence of star dunes within the Rub' Al-Khali and Dahna Deserts reveals the existence of another paleowind direction, which influenced the formation of these dunes.

Coarse mean grain sizes in the Hail and Tayma locations may be the result of rock fragments from the basement and the Paleozoic sedimentary rocks surrounding the sand dunes. The fine mean grain sizes in sand dunes from the Sakaka area reflect long distance from the sediment source (basement and Paleozoic sedimentary rocks outcrop). Fine mean grain sizes in sand dunes from the Red Sea reflect the effect of alluvial fans on sediment supply. The fine-grained sands of dunes in the eastern part of UAE (Al-Sayed 1999) are similar to sand dunes in the Rub' Al-Khali and Sakaka area deserts of Saudi Arabia. The average sorting value in this study is 0.79 Phi, which is similar to the average sorting value identified in the An Nafud Desert in Saudi Arabia (0.87) (Binda 1983). These values are different from the average value for sand dunes in UAE (0.43 Phi) and Oman (0.22 Phi) (Al-Sayed 1999). Thus, the sand dunes in Oman and UAE showed sorting better than those in Saudi Arabia, which reflects long distances from sediment source areas. Sand dunes from the Red Sea are poorly sorted, which reflects the short distance of sand transport. The average mean grain size and sorting for sand dunes in Saudi Arabia are 1.72 and 0.81 Phi, respectively. These values are similar to the average mean grain size and sorting identified in the Kumtagh Desert dunes in NW China, which are 1.57 and 0.71 Phi, respectively (Liu et al. 2014). However, the average grain size and sorting value in the Altar Desert in NW Mexico are 2.07 and 1.0 Phi, respectively (Kasper-Zubillaga et al. 2007). These sands are finer and less sorted than dune sands in Saudi Arabia. Moreover, the average mean grain size found in Namibian and southern Angolan dunes is almost similar to the medium mean grain size of Arabian desert sand dunes (Garzanti et al. 2015).

Dune sand grains from the Red Sea, Qassim, central Arabia, and the Eastern Province are characterized by subangular edges, which indicates that these dunes sands were deposited near to their source region. Other locations are characterized by subrounded sand grains, which reflect long transport pathways. Red Sea dune sand grains showed more angularity than the other dune sands, which indicates a shorter sediment transport distance and the close proximity of the depositional site to its sediment source. However, Rub' Al-Khali, as well as Najran dune sand grains, were more rounded than grains from other locations, which reflects the longest transport pathway and illustrates the effect of wind in transportation. In comparison with the other sand dunes on the Arabian Peninsula, the sand dunes in UAE have the most rounded grains, which reflect an extensive transportation by wind (Al-Sayed 1999).

SEM microphotographs of sand grains from the different areas in Saudi Arabia showed the presence of mechanical and chemical features on grain surfaces. Mechanical V-shaped pits reflect the impact of subaqueous environments (fluvial, littoral, and shelf environments) (Margolis and Krinsley 1974). V-shaped pits caused by mechanical processes usually occur in moderate- to high-energy conditions. Meandering ridge features characterize dune sands in the Red Sea area. These meandering ridges were likely formed during grain to grain collision in an eolian environment; thus, they indicate transportation by a high velocity wind (Kasper-Zubillaga and Faustinos-Morales 2007). Upturned plates characterize dune sand grains from the Najran, central Arabia, Qassim, and Sakaka locations. Upturned plates are often developed in eolian environments (Mazullo and Ehrlich 1983). Therefore, these sand dunes developed in an eolian environment with high-velocity winds (Mazullo et al. 1986). Solution pits in dune sands from the Sakaka, Tayma, and Tabuk locations reflected chemical processes in tropical areas, like the intertidal zone of a beach (Kasper-Zubillaga and Faustinos-Morales 2007) (Higgs 1979).

The immature state of the basement-related sand dunes in Najran (N1), central Arabia (C5), and the Red Sea reflects the immaturity of the sediment source and the short transportation. On the other hand, the mature state of sand dunes not related to basement rocks may be due to a high recycling rate of sediments and/or a sediment source being far from the depositional basin. Mineralogical and geochemical similarities between the basement-related sand dunes in Najran (N1), the Red Sea, and central Arabia (C5) likely reflect similarity of the source rocks and the weathering history. In contrast, the sediments recycling, and the media and pathway of transportation may also affect the mineralogical and chemical properties of such sand dunes.

The mineral composition of dune sands from the northwest Rub' Al-Khali is similar to the mineral composition of dune sands in the western part of Rub' Al-Khali (Moufti 2013). Thus, the northwest and the west Rub' Al-Khali dune sands likely reflect similar source rocks.

Conclusions

1. Morphologically, sand dunes in Saudi Arabia vary from linear, parallel to subparallel, parabolic, barchans, and star sand dunes.
2. The variability in sand dune types reflects the varied paleowind direction during the evolution of sand dunes and associated climatic changes.
3. The interested sand dunes show variation in texture and mineralogical composition. This variation is attributed to different sediment sources, geology, varied transportation modes and distances, weathering, depositional processes, and climatic changes.
4. Nonbasement-related sand dunes are texturally moderately mature and quartz arenitic in composition. However, basement-related sand dunes are submature and subarkosic to litharenitic in composition.
5. Major, trace, and rare earth elements geochemistry indicated that the most of the eolian sand dunes are quartz arenite, except the sand dunes from the Red Sea, central Arabia (C5), and Najran (N1) (all basement-related), which are subarkose to litharenite.
6. Discriminant analyses and bivariate plots of the elemental geochemistry indicated that Red Sea, Najran, and central Arabian sand dunes are underlain by active continental margins, and sand dunes from other areas are underlain by passive continental margins.
7. The finding of this study shows that major, trace, and rare earth element distribution can be used to differentiate between basement-related and nonbasement-related derived sand dunes.
8. The study of recent sand dunes can help to understand and predict detrital sources and their textural and compositional characteristics, along with those sources' impacts on any sand dunes' economic potential (i.e., reservoirs, aquifers, and mineral deposits).

Acknowledgments We would like to thank the Earth Sciences Department and Research Institute of KFUPM for support and assistance provided for field and laboratory studies. In addition, thanks are due to Mr. Mushabab Asiri, Mr. Aziz Khan and Abdullah AlQubalee for their great effort on lab analysis.

References

Abolkhair Y (1986) The statistical analysis of the sand grain size distribution of Al-Ubay-lah barchan dunes, northwestern Ar-Rub-Alkhali Desert, Saudi Arabia. GeoJournal 13(2):103–109

Al-Dousari AM, Al-Enezi AK, Al-Awadhi J (2008) Texture variation within different representative types of dune sediments in Kuwait. Arab J Geosci 1(1):17–31

Al-Masrahy MI, Mountney NP (2013) Remote sensing of spatial variability in aeolian dune and interdune. Aeolian Res 11:155–170

Al-Sayed MI (1999) Sedimentological characteristics and morphology of the aeolian sand dunes in the eastern part of the UAE: a case study from Ar Rub' Al Khali. Sediment Geol 123(3):213–239

Anton D (1983) Modern eolian deposits of the Eastern Province of Saudi Arabia. Dev Sedimentol 38:365–377

Bhatia M (1983) Plate tectonic and geochemical composition of sandstone. J Geol 91:611–622

Bhatia M, Crook K (1986) Trace element characteristics of graywackes and tectonic setting discrimination of sedimentary basins. Contrib Mineral Petrol 92(2):181–193

Binda PI (1983) on the skewness of some aeolian sands from Saudi Arabia. Dev Sedimentol 38:27–39

Blount G, Lancaster N (1990) Development of the Gran Desierto sand sea. Geology 18:724–728

Edgell H (2006) Arabian deserts: nature, origin and evolution. Springer, Dordrecht

Folk R (1974) Petrology of sedimentary rocks, 2nd edn. Hemphill press, Austin

Fryberger SG, Al-Sari AM, Clisham TJ, Rizvi SA, Al-Hinai KG (1984) Wind sedimentation in the Jafurah sand sea, Saudi Arabia. Sedimentology 31(3):413–431

Garzanti E, Ando S, Vezzoli G, Dell'Era D (2003) From rifted margins to foreland basins: investigating provenance and sediment dispersal across desert Arabia (Oman, U.A.E.). J Sediment Res 73(4):572–588

Garzanti E, Vermeesch P, Ando S, Vezzoli G, Valagussa M, Allen K, Kadi K, Al-Juboury A (2013) Provenance and recycling of Arabian desert sand. Earth Sci Rev (120):1–19

Garzanti E, Resentini A, Ando S, Vezzoli G, Pereira A, Vermeesch P (2015) Physical controls on sand composition and relative durability of detrital minerals during ultra-long distance littoral and aeolian transport (Namibia and southern Angola). Sedimentology 62(4): 971–996

Herron MM (1988) Geochemical classification of terrigenous sands and shales from core or log data. J Sediment Petrol 58(5):820–829

Higgs R (1979) Quartz grain surface features of Mesozoic–Cenozoic sands from the Labrador and Western Greenland continental margins. J Sediment Petrol 49:599–610

Ingram RL (1971) Seive analysis. In: Carver RE (ed) Procedures in sedimentary petrology. John Wiley and Sons, New York, pp 49–67

Issautier B, Le Nindre YM, Memesh A, Dini S, Viseur S (2012) Managing clastic reservoir heterogeneity. I: sedimentology and sequence stratigraphy of the Late Triassic Minjur Sandstone at the Khashm al Khalta type locality, Central Saudi Arabia. GeoArabia, J Middle East Pet Geosci 17(2):17–56

Kasper-Zubillaga J, Carranza-Edwards A (2005) Grain size discrimination between sands of desert and coastal dunes from northwestern Mexico. Rev Mex Cienc Geol 22:383–390

Kasper-Zubillaga JJ, Faustinos-Morales R (2007) Scanning electron microscopy analysis of quartz grains in desert and coastal dune sands (Altar Desert, NW Mexico). Cienc Mar 33:11–22

Kasper-Zubillaga J, Zolezzi-Ruíz H, Carranza-Edwards A, Girón-García P, Ortiz-Zamora G, Palma M (2007) Sedimentological, modal analysis and geochemical studies of desert and coastal dunes, Altar Desert, NW Mexico. Earth Surf Process Landf 32(4):489–508

Kenneth P, Haim T (2009) Aeolian sand and sand dunes. Springer, Berlin

Le Nindre YM, Vaslet D, Le Métour J, Bertrand J, Halawani M (2003) Subsidence modelling of the Arabian Platform from Permian to Paleogene outcrops. Sediment Geol 156(1):263–285

Liu B, Qu J, Ning D, Gao Y, Zu R, An Z (2014) Grain-size study of aeolian sediments found east of Kumtagh Desert. Aeolian Res 13:1–6

Margolis S, Krinsley D (1974) Processes of formation and environmental occurrence of microfeatures on detrital quartz grains. Am J Sci 274: 449–464

Mazullo J, Ehrlich R (1983) Grain shape variation in the St. Peter Sandstone: a record of eolian and fluvial sedimentation of an Early Paleozoic cratonic sheet sand. J Sediment Petrol 53:105–119

Mazullo J, Sims D, Cunningham D (1986) The effects of eolian sorting and abrasion upon the shapes of fine quartz sand grains. J Sediment Petrol 56:45–56

Moufti M (2013) Mineralogy, geochemistry and possible provenance of desert sand dunes from western Rub' al Khali area, southeastern Saudi Arabia. Int J Basic Appl Sci 2(4):399–407

Muhs DR (2004) Mineralogical maturity in dune fields of North America, Africa and Australia. Geomorphology 59:247–269

Pease P, Bierly G, Tchakerian V, Tindale N (1999) Mineralogical characterization and transport pathways of dune sand using Landsat TM data, Wahiba Sand Sea, Sultanate of Oman. Geomorphology 29(3): 235–249

Phillips JA (1982) The red sands of the Arabian desert. Q J Geol Soc Lond 38(150):110–113

Preusser F, Radies D, Driehorst F, Matter A (2005) Late Quaternary history of the coastal Wahiba Sands, Sultanate of Oman. J Quat Sci 20(4):395–405

Roser BP, Korsch RJ (1988) Provenance signatures of sandstone–mudstone suites determined using discriminant function analysis of major-element data. Chem Geol 67:119–139

Sagga A (1998) Barchan Dunes of Wadi Khulays, Western Region of Saudi Arabia: geomorphology and sedimentology relationships. J K A U Earth Sci 10:105–114

Wang X, Dong Z, Zhang J, Zhao A (2003) Grain size characteristics of dune sands in the central Taklimakan Sand Sea. Sediment Geol 161: 1–14

Watson A (1986) Grain-size variations on a longitudinal dune and a barchan dune. Sediment Geol 46(1):49–66